Ab Initio Periodic Hartree−Fock Calculations for Interpretation of the Scanning Tunneling Microscope (STM) Images of Graphite

Kee Hag Lee*,†, M. Causá*,‡, and Sung Soo Park†

Department of Chemistry, WonKwang University, Iksan 570-749, South Korea, and Department of Chemistry IFM, University of Torino, Via P. Giuria 5, Torino 10125, Italy

Received: January 6, 1998; In Final Form: April 24, 1998

By using the CRYSTAL95 program, ab initio periodic Hartree−Fock (PHF) calculations with the full potential and 6-21G* basis set are applied to interpretation of scanning tunneling microscope (STM) images on hexagonal graphite. Our results show asymmetry similar to the experimental and previous pseudopotential calculations. The dominant feature is the deep hollow in the middle of the carbon hexagon. The three carbon atoms that do not have a neighbor in the second layer appear as small hills, the other three with neighbors in the second layer simply appear as saddle points. Our calculation has been successfully used to reproduce experimental features such as the effect of increasing the magnitude of the bias voltage and the effect of increasing the tip-to-surface separation.

Introduction

Scanning tunneling microscopes (STMs) are used to obtain surface images and spectra with atomic scale resolution for metals, semiconductors, and superconductors in real space.[1] Surface science has profited remarkably from the ability of STMs to map the surface atomic and electronic structure directly in real space.

Tersoff and Hamann[2] have shown that, under reasonable simplifying approximations, the STM topography is a map of constant charge density at $E_{F.}$ It has been made clear that the corrugation seen in an STM experiment is not necessarily that of the total valence electron charge; rather, it is closer to that of the local density of the states. After applying a bias voltage V, a tunneling current flows from the occupied electronic states near the Fermi level E_F of one electrode into the unoccupied states of the other electrode. The energy range is given by the bias voltage applied across the tunnel gap because only the states in the energy window $E_F \pm eV$ contribute to the tunneling current. The total electron density corrugation and the local density corrugation seen by the STM, however, begin to look very different in the presence of a gap or pseudogap as in semiconductors or semimetals.[3]

Layered materials, such as graphite and transition metal dichalcogenides, are especially attractive as STM substrates for atomic scale imaging. These surfaces have been extensively imaged because it is easy to prepare atomically flat regions over thousands of square angstroms.[4] The surfaces can be examined in air and in liquids free of the effects of contamination. The crystal structure of the surface of layered materials studied to date is either a trigonal or a honeycomb lattice.

The crystal structure of graphite is hexagonal with symmetry group D_6^h. The nearest-neighbor distance in each honeycomb is 1.42 Å, whereas the spacing between layers is 3.35 Å. There is a hollow in the middle of the unit hexagon (site H). The carbon atom at site A has a neighboring atom in the second layer. The atom at site B does not have the underlying atom.

STM has been used to image the surface of graphite with atomic resolution in UHV,[3] air,[4−6] and water[6,7] with similar results. The most definitive study was carried out by Binnig et al.[4] in a UHV station. These authors reported the hexagonal structure of the surface layer, which shows an asymmetry in the charge density of neighboring atoms and a clear manifestation of such an energy-dependent corrugation. A large apparent asymmetry leading to the resolution of only every other atom in most STM images[3−7] is unexpected because the week interaction between layers should ensure that the total charge densities on these atoms are almost identical. But it should not be surprising that, in systems with a Fermi surface containing a limited number of states of specific character, such as graphite, the observed images can look very different from what the atomic (or total charge density) structure would suggest.

Selloni et al.[8] used empirical, not norm-conserving pseudopotential, and a four-layer graphite slab model to study wave function properties. They pointed out that graphite provides an ideal testing ground for an energy-dependent corrugation seen by STM. By calculating the current−voltage characteristics, they predicted that the STM corrugation of graphite would drop with increasing tunneling voltage, V, at the tip-to-separation, d, of 2.5 Å.

Tersoff [9a] has presented an analysis of unusually high corrugations observed in STM images of 1T-TaS_2, Si (111)(2 × 1), and graphite. They show unusual corrugations to be characteristic of materials where the Fermi surface has collapsed to a point at the corner of the surface Brillouin zone, using a monolayer of graphite and plane wave functions. Although this work[9a] is interesting theoretically, it is not believed to be correct. The most likely reason for the giant corrugation sometimes observed on graphite surface is due to a carbon whisker that forms at the end of the tip.[9b,c] This whisker acts as a tip and behaves like a weak spring element. 1T-$TaSe_2$ has a half-filled band, and its Fermi surface is not collapsed to a k-point. Nevertheless, its STM image exhibits a large corrugation.[9d] The

* To whom correspondence should be addressed. E-mail address: khlee@wonnms.wonkwang.ac.kr or causa@ch.unito.it. Fax for Kee Hag Lee: -82-653-850-7312.
† WonKwang University.
‡ University of Torino.

S1089-5647(98)00639-7 CCC: $15.00
Published on Web 07/15/1998

reason for this large corrugation was well explained in terms of local density of states of the surface contributed by the electrons near the E_F.

Batra et al.[10] used the self-consistent pseudopotential method within the local density functional theory and a three-layer graphite slab to interpret the STM image of graphite. The pseudopotential method with plane wave basis is ideally suitable for calculating the electronic structure of a graphite surface, as long as a large number of plane wave basis are used. Although they used relatively smaller kinetic energy cutoff of 18 Ry with some modified plane wave basis, they were able to successfully employ it for drawing the asymmetry of graphite. They suggest that by going from the center of the hexagon to the surrounding atoms, the site that does not have a subsurface atom below yields higher corrugation.

Tománek et al.[11,12] reported that asymmetry at each carbon atom is nearly independent of the polarity and decreases with increasing magnitude of the bias voltage: site A (saddle point), site B (small hill), and site H (deep hollow). The electron energies and wave functions were obtained by solving ab initio pseudopotential local orbital method within the density functional formalism. For each site, they considered 12 independent basis functions, which were complemented by four long-range Gaussians, located at half the interlayer distance above and below each carbon atom. They found that extending the local basis set with floating orbital sites in the interlayer region does not modify their STM results.

With an extended Hückel tight-binding calculation Whangbo et al.[13a,b] reported structural and electronic properties of graphite and graphite intercalation compounds MC_8 (M = K, Rb, Cs) governing their STM images. They showed that graphite STM images reflect both the electronic and mechanical effects.

Experimental STM data[1,3,14,15] showed other significant results also: for example, the absence of trigonal symmetry and the giant corrugation. Giant corrugation has been attributed to a geometric effect, which is tip-induced deformation of a graphite layer during low resistance tunneling.[14,15] In this paper, we consider electronic effect, with a focus on the asymmetry of a carbon site with increasing magnitude of the bias voltage and the tip-to-surface separation.

Theoretical Approach

We used ab initio periodic Hartree−Fock (PHF) calculations in the CRYSTAL95 program[16] with 6-21G* basis set[17] and a graphite slab model with three layers.[18]

Applying a small bias voltage V between the tip and the sample yields a tunneling current. The ideal STM would have the greatest possible resolution and would measure the intrinsic properties of unperturbed surfaces rather than the properties of the joint surface−tip interface. A tip whose potential and wave functions were arbitrarily localized would best achieve this ideal condition. In that case, Tersoff and Hamann[2] have considered the limit of the point probe. In the small bias voltage limit, the tunneling conductance, σ is

$$\sigma \propto \rho_{STM}(r, V) \tag{1}$$

where

$$\rho_{STM}(r, V) \equiv \int_{E_F - eV}^{E_F} dE \rho(r, E) \tag{2}$$

and

$$\rho(r, E) \equiv \sum_v |\psi_v(r)|^2 \delta (E_v - E) \tag{3}$$

where r is in the position of the center of curvature of the tip s state, E_F is the Fermi energy, $\rho(r, E)$ is the surface local density of states (LDOS) of the bare surface at the center of curvature of the tip $r = (x, y, z)$ and $\psi_v(r)$ are the electron eigenstates of the unperturbed surface with corresponding energy E_v. For a periodic system, the sum of the v states is a sum of the bands and an integral of the k space spanning the irreducible part of the Brillouin zone. In CRYSTAL95, a regular mesh of interpolating points is used for performing the numerical integration in the reciprocal space. In the present calculation of graphite, each axis of the two-dimensional unit cell of the reciprocal space is subdivided into 12 parts, giving a symmetry irreducible set of 31 sampling k points (symmetry equivalent to 150 k points).[19] In each point, eigenvalues and eigenvectors are calculated. Then, the energy bands are interpolated by a direct-space Fourier series, and the values in a denser sampling net are calculated to be used for evaluating the energy integral in eq 2. In the present calculation, a set of 109 k points (symmetry equivalent to 500 k points) is used in the interpolated net. The details of the k integration scheme can be found in ref 20. The implied assumptions[7−9] are that the description of the relevant tip states is by a locally spherical potential well with a constant density of states where it approaches nearest to the surface with a constant density of states, and that the tunneling matrix element is independent of the lateral tip position for a constant tip-to-position and also is independent of the bias voltage V in the narrow energy region $[E_F \pm eV, E_F]$.

The calculation of STM charge density, $\rho_{STM}(r, V)$ is performed by sampling the k-space region near the Fermi surface in the irreducible part of surface Brillouin zone (BZ). Not all the k points contribute to $\rho_{STM}(r, V)$, because the portion of the band structure sampled by the STM is very small for typical tunneling voltages below ~1 V. Here, we calculate the STM charge density within bias voltages of 0.5, 1.0, and 1.5 V, respectively. The STM charge densities at bias voltages of 0.5 and 4.0 V at the tip-to-surface separations (d) of 1.0 and 4.0 Å, respectively, are represented in Figure 1.

The current densities in previous experiments[1,3,11] and calculations[1c,8,10−13] have shown asymmetry at each carbon site in graphite. Our results also show considerable asymmetry between sites A and B for tunneling voltages of 0.5 and 4.0 V as shown in Figure 1. The dependence of the tunneling current density on the bias voltage for graphite, which shows a strong decrease of the asymmetry with increasing bias voltage, is also demonstrated in Figures 1 and 2. This behavior can be quantified by defining the asymmetry[12] A between the STM charge densities at site A and site B by

$$A = (\rho_{STM}(B) - \rho_{STM}(A))/(\rho_{STM}(B) + \rho_{STM}(A)) \tag{4}$$

The bias voltage dependence of A for the surface of graphite is shown in Figure 2 for eight different tip-to-surface separations (1.0−7.0 Å) at three different bias voltages (0.5, 1.0, 1.5 V). Our results indicate no strong dependence of the asymmetry on the tip-to-surface separation in the range 1.0−7.0 Å, but there is a strong decrease of the STM charge density in this range.

Results and Discussion

The interpretation of the observed tunneling current σ in terms of local densities of states as shown in eq 1 is based on several assumptions, which may be an oversimplification of the real experimental situation. Here, we calculate STM charge densities $\rho_{STM}(r, V)$ defined in eq 2. For both a constant tip-to-surface separation with low bias voltages and a constant low bias voltage

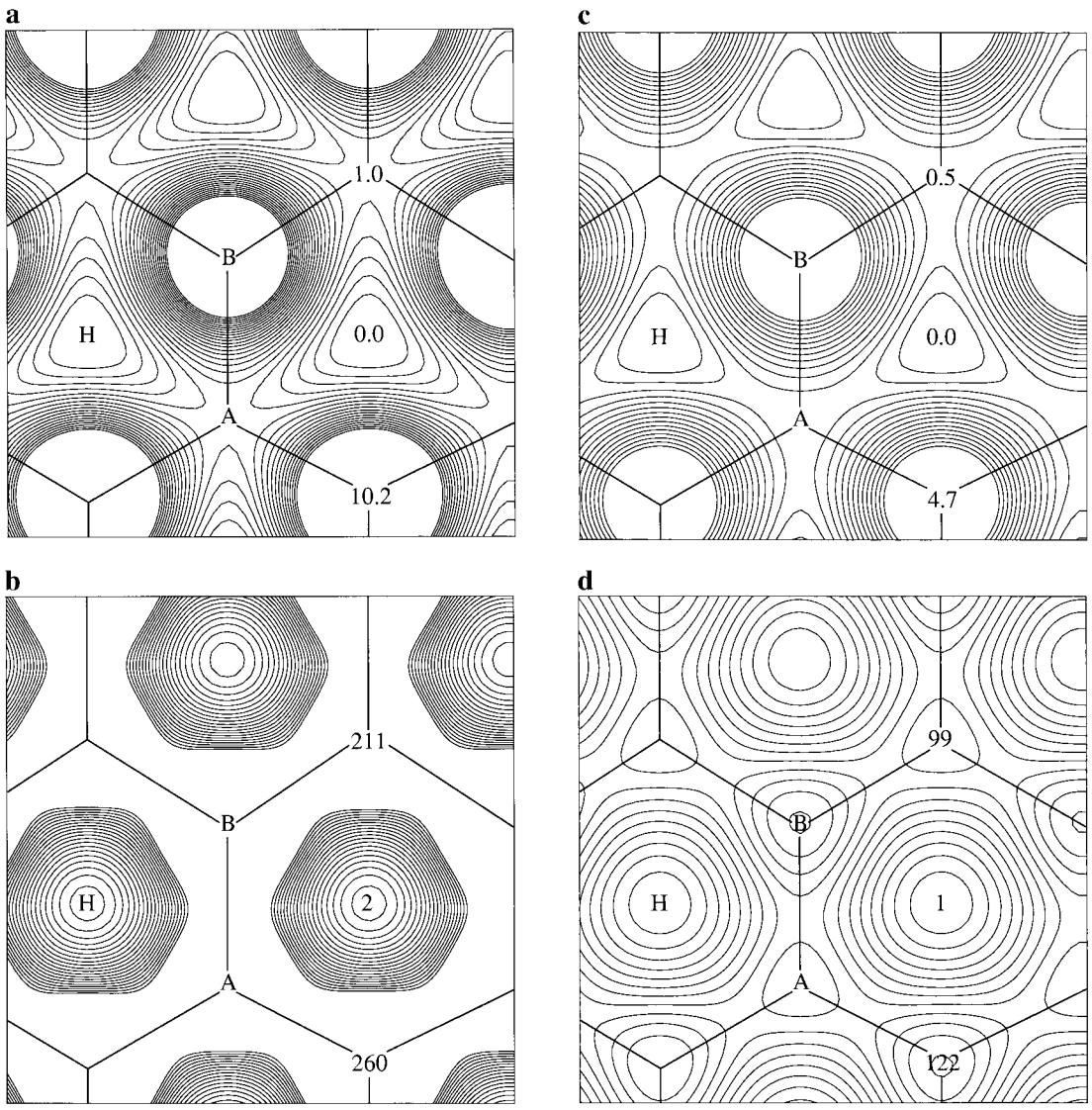

Figure 1. Contour plots of the STM charge density ρ_{STM} in plane parallel to and 1 and 4 Å above the topmost surface layer. Surface results for ρ_{STM} with the tip-to-surface separation 1 Å are given for bias voltages (a) $V = 0.5$ V and (b) 4.0 V. The units are 10^{-5} electrons/au^3, and consecutive contours from minimum isolines are separated by (a) 0.2×10^{-5} and (b) 5×10^{-5} electrons/au^3, respectively. Surface results in (c) and (d), with the tip-to-surface separation 4 Å, are obtained for the same bias voltage as (a) and (b), respectively. The results are given in units of 10^{-14} electrons/au^3, with consecutive contours from minimum isolines separated by 0.2×10^{-14} and 10×10^{-14} electrons/au^3 in (c) and (d), respectively.

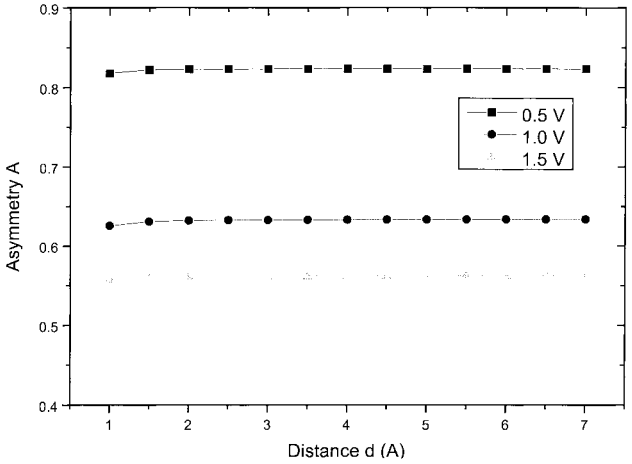

Figure 2. Results of ab initio PHF calculations for the dependence of asymmetry A of the STM charge density for the surface of graphite on the tip-to-surface separation d for bias voltages 0.5, 1.0, and 1.5 V.

with tip-to-surface separation, the tunneling matrix element, which determines the proportionality constant in eq 1, is assumed to be not very sensitive to the lateral tip position. Then, STM charge densities $\rho_{STM}(r, V)$, calculated in planes parallel to the surface may be compared with the relative changes in the tunneling current σ observed in the current imaging (constant distance) mode.

There are two reasons for the asymmetry of graphite STM images, as already discussed in the literature,[1c,13] which are both electronic and mechanical effects. The electronic effect is that the interlayer C·····C interaction makes the orbitals around the Fermi level more concentrated on the B-site carbon atoms. The Fermi level happens to occur around the K point for highly oriented pyrolytic graphite (HOPG). The mechanical reason is that the tip-force-induced surface corrugation makes the B site carbon atoms more elevated than the A-site carbon atoms. However, here we consider only the electronic effect of graphite STM images with the ab initio PHF calculations. As before, we also find that the observed asymmetry between neighboring carbon sites on graphite originates from the special symmetry of the electronic states near the K point in the surface BZ. Our calculations also show, as before, that the general trend of decreasing A in eq 4 with increasing V holds even for large

negative bias voltages, corresponding to tunneling into an unoccupied graphite state, as confirmed by the work of Tománek et al.[11] Whangbo et al.[13] explained why this situation should be so in terms of the orbital interaction theory that the p_π orbitals of the *A* sites have σ interactions through the interlayer C····C contacts, whereas those of the B sites experience no such interactions.

Tománek et al.[11,12] reported that the STM images and observed asymmetries can vary considerably for different tips and samples. By using the density functional formalism with the pseudopotential they obtained the theoretical asymmetry within bias voltages from ∼0.1 to 0.8 V at the tip-to-surface separation $d = 0.5$ and 1.0 Å. Because a finite lateral imposes an upper limit on the maximum value of the observable asymmetry, they expected the observed asymmetry to be smaller than the calculated values, which correspond to an infinitely sharp tip. They showed that this expectation is consistent with the result of comparing theoretical and experimental data, especially in the bias voltage range corresponding to large asymmetries. Also, at substantially larger distances to the surface (few angstroms), that might correspond to realistic tip-to-surface separations, they estimated how the tip-to-surface separation from 1.0 to 7.0 Å affects STM charge densities on the bias voltage range (0.2−0.8 V) at the tight-binding level. Thus, we were interested in determining how the tip-to-surface separation from 1.0 to 7.0 Å affects STM charge densities on the bias voltage range (0.5−1.5 V) at the ab initio PHF level.

As shown in Figure 1, we obtained the asymmetries for STM charge densities on the bias voltages 0.5 and 4.0 V. The result suggests that the corrugation of the charge density owing to the states around the Fermi level is larger than that of the total valence charge density. This result agrees with previous works.[1c,10−13]

As shown in Figure 2, we obtained the asymmetries for STM charge densities on the bias voltage range 0.5−1.5 V at the tip-to-surface separation $d = 1.0$−7.0 Å by ab initio PHF calculations with the full potential and the 6-21G* basis set. Calculated asymmetries are larger than the observed values and there is a very noticeable trend of decreasing asymmetry with increasing the bias voltages (Figure 2). Our results have the same tendency as those of Tománek et al.,[12] but our calculated asymmetries on the STM charge densities are larger than their results. As an example, at bias voltage $V = 0.5$ V and the tip-to-surface separation $d = 1.0$ Å, our calculated asymmetry value on the STM charge density is ∼6 times larger than their result obtained from the density functional formalism with the pseudopotential.

The tip-to-surface separation in the experiment is not accurately known, so we performed our calculations for the tip-to-surface distances $d = 1.0$−7.0 Å and found small changes in the asymmetry *A*. At substantial distances to the surface, which might be within the realistic tip-to-surface separations, *A* is not expected to decrease. But, by the time the tip-to-surface distance is beyond 4 Å, the absolute values of the local density on the A and B sites are so small that it would not be meaningful to talk about their difference. Also in STM experiments, the radius of a typical Pt/Ir STM tip is ∼10 nm and the radius a Pt or Ir atom at the tip end is ∼2.5 Å. Thus, once the tip-to-surface distance is beyond several angstroms, the numbers with the point-tip approximation in this work would be meaningless. Also, our results agree with the literature[2,8,9] that the STM charge density at each site at substantially larger distances is expected to decrease. This result shows that the STM charge density decreases by the exponential dependence on distance.

By using the tight-binding model, Tománek et al.[12] showed that with increasing bias voltages, states from an increasingly large portion of the surface BZ contribute to the STM charge density. This contribution causes smoothing of the STM charge density due to those states and, as a consequence, a reduction of the asymmetry as well as a more rapid decrease in asymmetry as a function of distance. As shown in Figure 2, our results also reflect a reduction of the asymmetry with increasing the bias voltage. But, as shown in Figure 2, asymmetry *A* on the STM charge density is not very dependent on the tip-to-surface separation, even though the STM charge density at each site is exponentially decreasing with increasing tip-to-surface separation.

Our ab initio PHF results with the full potential and 6-21G* basis set agree with previously published density functional and tight-binding results, thus supporting previous theoretical results. The present work is the first ab initio PHF calculation to interpret the STM image for graphite.

Acknowledgment. This work was supported by the Ministry of Education (BSRI-97-3438) and the Ministry of Science and Technology (1996), Korea. We thank the reviewer for the very valuable comments and Prof. H. Kang at POSTECH for stimulating discussions.

References and Notes

(1) (a) Wiesendanger, R. *Scanning Probe Microscopy and Spectroscopy*; Cambridge University: Cambridge, 1994. (b) Wiesendanger, R.; Anselmetti, D. *Surface Properties and Layered Structures*; Kluwer: Dordrecht, The Netherlands, 1992; p 1. (c) Magonov, S. N.; Whangbo, M.-H. *Surface Analysis with STM and AFM*; VCH: Weinheim, Germany, 1996.

(2) (a) Tersoff, J.; Hamann, D. R. *Phys. Rev. Lett.* **1983**, *50*, 1998. (b) Tersoff, J.; Hamann, D. R. *Phys. Rev. B* **1985**, *31*, 805.

(3) Binnig, G.; Fuchs, H.; Gerber, Ch.; Rohrer, H.; Stoll, E.; Tosatti, E. *Europhys. Lett.* **1986**, *1*, 31.

(4) Baro, A.; Miranda, R.; Alaman, J.; Garcia, N.; Binnig, G.; Rohrer, H.; Gerber, Ch.; Carrascosa, J. L. *Nature* **1985**, *315*, 253.

(5) Park, S.-I.; Quate, C. F. *Appl. Phys. Lett.* **1986**, *48*, 112.

(6) Schneir, J.; Sonnenfeld, R.; Hansma, P. K.; Tersoff, J. *Phys. Rev. B* **1986**, *34*, 4979.

(7) Sonnenfeld, R.; Hansma, P. K. *Science* **1986**, *232*, 211.

(8) Selloni, C. A.; Carnevali, P.; Chen, G. D.; Tosatti, E. *Phys. Rev. B* **1985,** *31*, 2602; *ibid*. Errata **1986**, *34*, 7406.

(9) (a) Tersoff, J. *Phys. Rev. Lett.* **1986**, *57*, 440. (b) Pethica, J. P. *Phys. Rev. Lett.* **1986**, *57*, 3235. (c) Mate, C. M.; Erlandsson, R.; McClelland, G. M.; Chiang, S. *Surf. Sci*. **1989**, *208*, 473. (d) Whangbo, M.-H.; Ren, J.; Canadell, E.; Louder, D.; Parkinson, B. A.; Bengel, H.; Magonov, S. N. *J. Am. Chem. Soc*. **1993**, *115*, 3760.

(10) Batra, I. P.; Garcia, N.; Rohrer, H.; Salemink, H.; Stoll, E.; Ciraci, S. *Surf. Sci*. **1987**, *181*, 126.

(11) Tom nek, D.; Louie, S. G.; Mamin, H. J.; Abraham, D. W.; Thomson, R. E.; Ganz, E.; Clarke, J. *Phys. Rev. B* **1987**, *35*, 7790.

(12) Tom nek, D.; Louie, S. G. *Phys. Rev. B* **1988**, *37*, 8327.

(13) Whangbo, M.-H.; Liang, W.; Ren, J.; Magonov, S. N.; Wawkuschewski, A. *J. Phys. Chem.* **1994**, *98*, 7602.

(14) Soler, J. M.; Baro, A. M.; Garcia, N.; Rohrer, H. *Phys. Rev. Lett.* **1986,** *57*, 444.

(15) Salmeron, M.; Ogletree, D. F.; Ocal, C.; Wang, H.-C.; Neubauer, G.; Kolbe, W.; Meyer, G. *J. Vac. Sci. Technol. B* **1991**, *9*, 1347.

(16) The periodic Hartree−Fock (PHF) method systematically expands the band structure, whereas the density functional theory (DFT) systematically underestimates band gaps and bandwidths. We calculated with our program both PHF and DFT and found qualitative agreements in the band structure for the two methods. We also found a qualitative agreement of the asymmetry in the charge density on sites A and B of graphite. Dovesi, R.; Saunders: V. R.; Roetti, C.; Causá, M.; Harrison, N. M.; Orlando, R.; Aprá, E. *CRYSTAL95 User's Manual;* University of Torino: Torino, Italy, 1996.

(17) We checked the stability of our results with the basis set, changing the external exponent in the range 0.19−0.27. We confirmed that the best exponent is 0.24, and the STM images have no difference in the interval 0.21−0.25. So, we have reasonably reproduced the decay of the density perpendicularly to the surface. The linear combination of atomic orbitals periodic calculations cannot use diffuse basis sets because the real basis is

the set of block functions built over the atomic orbitals: too wide functions give linear dependence between the block functions. Gordon, M. S.; Binkley, J. S.; Pople, J. A.; Pietro, W. J.; Hehre, W. J. *J. Am. Chem. Soc.* **1982,** *104,* 2797.

(18) Our results are stable with the number of layers in the slab. We explored slabs composed of 2, 3, 4, and 5 graphite layers. The physical origin of the asymmetry in the graphite STM images is in the exchange short-range repulsion between the layers. Even a two-layer slab shows this interaction.

(19) Our results are stable with respect to the integration in the *k* space. We also obtain the same STM image using 2304 *k* points in the primary net and 20 736 *k* points in the interpolated net that we used for calculating the occupied fraction of the Brillouin zone for each energy value.

(20) (a) Pisani, C.; Dovesi, R.; Roetti, C. *Hartree−Fock ab initio Treatment of Crystalline Systems;* Springer-Verlag: Heidelberg, 1988. (b) Pisani, C.; Aprá, E.; Causá, M. *Int. J. Quantum. Chem.* **1990**, *38*, 395. (c) Pisani, C.; Aprá, E.; Causá, M.; Orlando, R. *Int. J. Quantum. Chem.* **1990,** *38,* 419.